Original Research Paper

IJES *Iranian Journal of Earth Sciences*
Vol. 15, No.2, 2023, 106-120.
DOI: 10.30495/ijes.2022.1935660.1634

Genesis and geochemical evolution of the Mio-Pliocene volcanic rocks in the SW of Bostanabad, NW Iran: A comparison with the classic Adakite

Farhad Pirmohammadi Alishah

Department of Geology, Shabestar Branch, Islamic Azad University, Shabestar, Iran

Received 17 June 2022; accepted 3 August 2022

Abstract

The Sahand volcano (Kuh-e-Sahand) is located in NW Iran, about 60 km E of Lake Urumieh and 40 Km SSE of Tabriz. The volcano is a stratovolcano and is dominated by pyroclastic materials and lava flows in the Miocene-Quaternary. The Mio-Pliocene volcanic rocks are exposed in the Southwest of Bostanabad (Arvanehkuh, Biukdagh, and Ghapandagh masses) East-Azerbaijan province. These rocks formed a part of the Urumieh-Dokhtar Magmatic Belt (UDMB) and consist of andesites and dacites. The rocks display a porphyritic texture and contain phenocrysts of plagioclase, sanidine, amphibole, biotite, and quartz. Based on the geochemical data and multi-elemental pattern, these rocks are medium to high-K calc-alkaline suite and show Large-Ion Lithophile Elements (LILE) and Light Rare-Earth Elements (LREE) enriched normalized multi-elemental patterns, and Nb and Ti depleted. Chondrite-normalized REE patterns of the volcanic rocks display a decrease from LREE to Heavy Rare-Earth Elements (HREE) without any Eu anomaly, indicating their formation in a subduction zone in an active continental margin. They have higher SiO_2, Sr content, Sr/Y, and La/Yb ratios and lower MgO, Y, and Yb contents compared to those of normal calc-alkaline volcanic rocks and show high SiO_2 adakites (HSA). Based on geochemical data, the origin of these rocks is garnet-amphibolite with the residual phase of garnet and amphibole with a titanium phase. HREE and Y depleted patterns suggest the existence of garnet and amphibole as a residue in the source. The source of these rocks was probably garnet-amphibolite possibly generated during subduction of the Neo-Tethyan oceanic slab beneath the Central Iran zone and in fact, can be termed as classic adakite. Therefore, considering the importance of adakites in inferring continental geodynamic processes, it is recommended to pay attention to their discovery and identification with the help of various petrological and geochemical methods.

Keywords: *Geochemistry, Dacite-andesite, Mio-Pliocene, Classic adakite, Urumieh-Dokhtar Magmatic Belt (UDMB)*

1. Introduction

In Iran, the main thrust of the Zagros is at the point of collision with the Central Iran plate. The northwest-southeast trend of the Urumieh–Dokhtar Magmatic Belt (UDMB) is parallel to the Zagros and Sanandaj-Sirjan zones with a width of 50 to 100 km and a length of 1800 km (Alavi 1994). Many geologists attribute the formation of the Urumieh-Dokhtar magmatic rocks to the subduction of the Neo-Tethys Ocean beneath the Iranian continental lithosphere (Berberian and Berberian 1981; Hassanzadeh 1993; Mohajjel et al. 2003) and believe that the Arabian plate collisions with Central Iran in the Upper Eocene-Late Miocene (Agard et al. 2011).

Various mechanisms have been proposed to justify magmatism in the UDMB, such as subduction zone melting, lower crustal melting due to infiltration of mantle magmas, partial melting of infiltration of the lower crust into subducted mantle wedges, and metasomatized by subduction fluid flux (Keskin 2003; Annen et al. 2006; Khodami 2019; Torkian et al. 2019; Vural and Kaygusuz 2021; Sipahi et al. 2021).

The findings of some researchers on magmatism after the impact of this magmatic belt also show that the melting of the submerged oceanic crust in the regions of this region has caused a large amount of adakitic magma (Jahangiri 2007; Ghadami et al. 2008; Omrani et al. 2008; Alishah et al. 2012; Bilici et al. 2020).

Although there is no consensus on the timing of the collision of the Arabian Plateau with central Iran, however, post-collision magmatic activity continued from the Late Miocene to the Quaternary (Ghasemi and Talbot 2005).

Today, Adakit refers to a large group of rocks with high La / Yb and Sr / Y ratios. This feature is due to processes such s: the melting of the oceanic crust, melting of the rich source of La and Sr, and weakness of Y and Yb. Also, with high concentrations of Sr and low Y and HREE and high ratios of Sr / Y and La / Yb, adakites were originally considered slab melting products in subduction zone settings. Adakites were therefore interpreted to provide information on magmatic processes, mineralization of economic reserves, and crustal evolution at convergent margins.

Adakites were therefore interpreted to yield information about magmatic processes, the mineralization of economic deposits, and crustal evolution along convergent margins (Jahangiri 2007; Ahmadzadeh et al. 2011; Aghazadeh et al. 2011; Noghreyan et al. 2011; Yadollahi et al. 2011; Alishah et al. 2012; Modjarrad 2013; Torkian et al. 2019).

All of these appear to be consistent with the UDMB. But their definite similarity needs further comparison and study. However, as more ‘adakites’ are reported, the lack of standardization of the term is becoming more apparent.

---

*Corresponding author.
E-mail address (es): Petrofarhad@iaushab.ac.ir

The uncertainty of the nomenclature mainly evolves from the breadth of lithological definitions and the diversity of proposed adakite genesis. This paper reviews progress on the definition of adakites and related concepts, and formally introduces widely used classifications and genetic models. In this study, the volcanic rocks of Arvanehkuh, Buokdagh, and Ghapandagh in the Mio-Pliocene age of the southwest of Bostanabad in East Azerbaijan province have been investigated. Observation of adakitic features in Mio-Pliocene (Neogene) magmatic rocks the southwest of Bostanabad has necessitated more attention to the origin and causes of magmatism in the region and the determination of its tectonic location. Therefore, the study focussed on finding the origin of the studied rocks based on recent field, petrographic, and geochemical findings.

2. Description of the study area

The study area is located northwest of the UDMB and East Azerbaijan province. The volcanic rocks of the southwest of Bostanabad are observed between the northern latitudes of 37˚ 35' to 37˚ 42' and Eastern longitudes of 46˚ 20' to 46° 30' between the cities of Bostanabad and Osco (Fig 1). Sahand volcano is adjacent to the active Tabriz Fault, and the alignment of its Quaternary volcanic structures broadly parallels the northwest-southeast trend of the Tabriz fault. Sahand's highest peak at 3,707 m elevation is one of 17 peaks higher than >3,000 m in this volcanic complex. Volcanic deposits of Sahand collectively cover an area of approximately 3,000 km^2, making it one of the laterally most extensive volcanic systems within the post-collisional volcanic province stretching During the Late Miocene, the first stratovolcano edifice of Paleo-Sahand formed from steeply dipping, alternating deposits of andesitic lava and pyroclastic rocks around a central crater (Ghalamghash et al. 2019; Ghaffari et al. 2013; Yazdi et al. 2022).

These volcanic deposits overlie Eocene volcanic and Paleozoic-Mesozoic sedimentary deposits including marine limestone and marl of the largely Lower Miocene Tethyan Qom Formation, along with continental deposits of the Middle-to Late Miocene Upper Red Formation at its southeastern flank (Davoudzadeh et al. 1997). During the Middle to Late Miocene, volcanoclastic deposits.

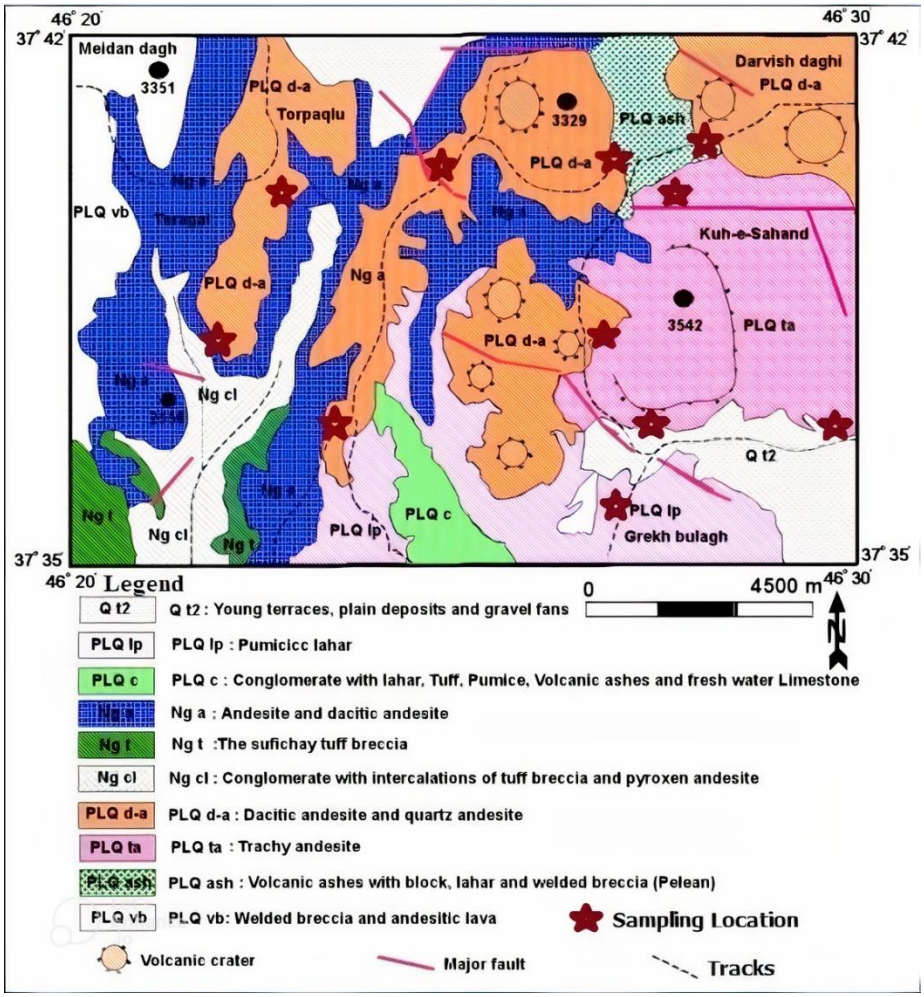

Fig 1. Study location and geologic map of the study area (Behrouzi et al. 1997).

derived from Sahand became intercalated with terrestrial basin-fill deposited in the Tabriz Basin to the northwest of Sahand volcano. These basin-fill sediments include up to 400 m thick lignite formations (Lignite Beds) and the overlying so-called Fish Beds, which represent lacustrine-palustrine deposits of up to 150 m in thickness consisting of tuffaceous mudstone, sandstone, tuff, and diatomite. The boundary between deposits of the Lignite Beds and Fish Beds is marked by a clear unconformity (Reichenbacher et al. 2011; Bina et al. 2020).

Pumice-rich tuff and pumiceous fall-out deposits up to 25–30 m in thickness are present in the middle part of the Lignite Beds and throughout the Fish Beds along the northern flank of the volcano. They attest to highly explosive conditions during the early stages of the evolution of Sahand. Along the southern and eastern flanks of Sahand volcano, Sahand volcanic deposits are interlayered with and overlying deposits of the Upper Miocene Maragheh (Ghalamghash et al. 2019).

2.1. Geology of the area

The most important magmatic rocks in this region are the Eocene volcanic and subordinate Neogene magmatism. The most important Neogene magmatic activity is the formation of the Oligo-Miocene intrusions and the volcanic domes with dacite-andesitic composition to the Miocene-Pliocene age (Amel 2008).

This region has been evaluated from the viewpoints of the sedimentary units by Stocklin and Setudenia (1971), Nabavi (1976), and Aghanabati (2004) in central Iran and the vicinity of the UDMB. The rocks of the region include dacite-andesitic volcanic and sub-volcanic domes that intersect with lava or dacite-andesitic rocks in different ages, including the Eocene volcanic, and reach the surface and form high altitudes (Fig 1). The volcanic activity of Sahand is characterized by the deposition of flat-lying ignimbrites. Collectively, deposits from sahand reach thicknesses >800 m (Moine Vaziri and Amine Sobhani 1977). The collapse of the volcanic rocks formed a major caldera, and ignimbrite deposits may be associated with this event. Younger volcanic activity successions within and outside the caldera boundaries. Lava domes form the prominent summits of Sahand, Boz, Darvish, and Sultan; smaller parasitic cones are Caban Dagh, Biouk Dagh, Arvaneh Dagh, Chahng Dagh, Cotor Dagh, and Ov Dagh. The areal extent of individual domes is limited to 5-15 km^2, and their deposits locally overlie the Sahand volcanic units mainly in the central and eastern areas of the complex. Several andesitic dikes intruded the Sahand volcanic deposits in the southwestern part of the Sahand volcano.

3. Sampling and Analytical Methods

To obtain information on the chemical composition of volcanic rocks Southwest of Bostanabad after microscopic examination of 50 thin sections, A total of 30 relatively fresh samples were collected from the rocks of the study area. The samples were among the fresh outcrops and the weathered rims of the samples were removed before packing in plastic sample bags. 10 samples after microscopic study, were analyzed for major, trace, and rare earth elements (REE) in the ALS Chemex Analytical Laboratory (Vancouver, Canada) by using ICP-MS (inductively coupled plasma mass spectrometry) after acid decomposition (Table 1). Major elements were determined by ICP-ES (inductively coupled plasma atomic emission spectrometry). Major element detection limits are about 0.001-0.2%. GIS Software (ArcMap) was used to draw the map and Minpet and Igpet Software were used for geochemical data analysis.

4. Results

4.1. Petrography

The investigated rocks include andesite and dacite. The dacites and andesites are more found as domes and lava flows, respectively (Fig 2). The main minerals of the dacites include plagioclase and hornblende which are both crystalline and fine-grained in the rock textures.

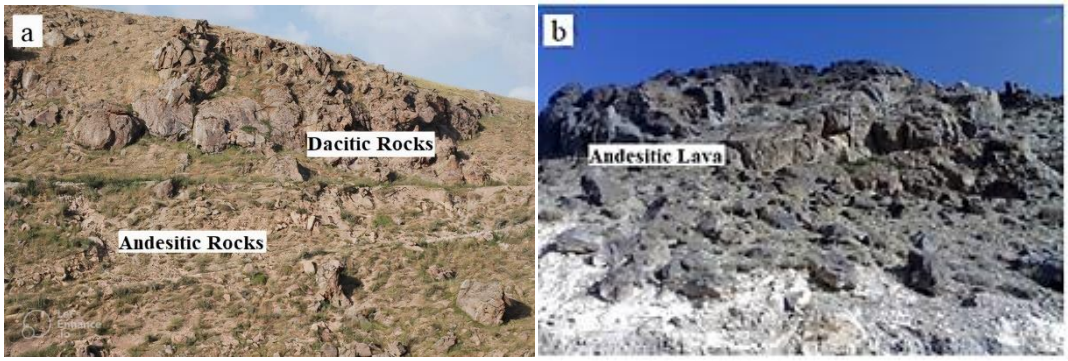

Fig 2. a) A view of the light-colored dacitic dome of the mountain Ervine and shrinkage seams in the Mio-Pliocene dacite-andesitic rocks of the southwest of Bostanabad, b) A view of an andesitic lava flow in the hot Buick Massif several meters thick on the volcanic Eocene flows.

Table 1. Chemical composition of the major (wt. %) and trace element (ppm) of the Mio-Pliocene dacite-andesitic rocks of the southwest of Bostanabad. $Fe_2O_{3(t)}$*0.899=FeO_t, Loss On Ignition(LOI).

Sample	D_1	D_2	D_3	D_4	A_1	D_5	D_6	D_7	D_8	A_2	A_3	D_9	A_4	D_{10}
Name	Dacite	Dacite	Dacite	Dacite	Andesite	Dacite	Dacite	Dacite	Dacite	Andesite	Andesite	Dacite	Andesite	Dacite
SiO_2 (wt. %)	65.72	64.91	65.35	65.65	58.2	63.15	65.55	64.72	64.1	58.45	57.81	66.45	58.20	64.35
Al_2O_3	15.65	15.9	15.75	16.25	17.5	16.25	16.25	16.05	16	15.1	15.65	16.65	15.8	15.95
FeO_t	2.58	3.12	3.25	2.56	3.55	3.62	2.86	2.69	3.21	3.42	3.29	2.87	3.52	2.74
Cao	2.76	3.09	2.79	3.68	6.17	3.66	3.57	3.27	3.59	4.49	3.38	3.75	4.28	3.81
MgO	1.01	1.73	1.35	1.12	2.63	0.78	1.08	2.36	1.15	2.42	2.15	2.98	2.85	1.46
Na_2O	4.72	4.25	5.12	4.43	3.68	4.90	5.01	4.90	4.25	4.37	4.2	4.62	3.44	4.45
K_2O	3.58	2.16	3.45	3.29	3.65	2.15	2.80	2.95	3.12	1.98	1.85	2.32	2.26	2.22
Cr_2O_3	0.01	0.01	0.02	0.03	0.01	0.02	0.02	0.01	0.01	0.01	0.01	0.02	0.02	0.02
TiO_2	0.31	0.25	0.32	0.41	0.66	0.4	0.38	0.27	0.38	0.27	0.37	0.45	0.38	0.38
MnO	0.03	0.03	0.03	0.05	0.13	0.04	0.05	0.03	0.06	0.03	0.05	0.05	0.05	0.06
P_2O_5	0.13	0.09	0.13	0.18	0.23	0.19	0.19	0.1	0.18	0.1	0.14	0.22	0.18	0.13
SrO	0.06	0.06	0.06	0.06	0.05	0.07	0.08	0.06	0.06	0.06	0.05	0.07	0.07	0.07
BaO	0.07	0.08	0.07	0.08	0.06	0.08	0.09	0.06	0.07	0.08	0.07	0.1	0.09	0.08
LOI	1.7	2.09	2.7	1.89	1.89	0.5	0.8	2.3	1.8	3.3	2.17	0.79	2.5	1.09
Total	99.5	100	99.7	99.6	99.5	99.4	99.9	99.5	100	99.8	100	100	100	100
Ba (ppm)	830	1026	950	752	750	689	762	538	617	654	608	839	713	704
Ce	1.12	0.95	1.02	1.42	2.35	5.32	2.36	5.35	3.64	4.36	4.62	6.23	4.36	6.32
Co	4.1	3.9	4.8	7.5	16.7	6.2	7.8	4.5	6.9	4.1	6.4	6.8	6.9	8.3
Cr	8	9	13	15	9	15	10	9	9	7	9	13	11	10
Cs	1.15	1.64	1.13	1.34	2.42	1.67	1.67	1.28	2.18	1.87	2.41	1.2	2.45	2.81
Cu	11	39	11	20	45	25	22	11	12	17	19	32	29	25
Dy	1.08	0.9	1.04	1.79	3.84	1.57	1.54	0.9	1.55	0.95	1.6	1.59	1.39	1.52
Er	0.5	0.43	0.48	0.92	2.39	0.81	0.85	0.45	0.83	0.48	0.81	0.78	0.7	0.75
Eu	1.14	1.31	1.15	0.93	1.13	1.14	1.11	1.21	0.98	1.25	1.1	1.16	1.13	0.99
Ga	18.4	17.5	18.7	19.1	18.3	19	18.9	17.2	18.4	17.6	18	19.5	18.1	18.9
Gd	2.38	1.93	2.35	3.05	4.53	2.85	2.71	1.63	2.6	1.96	2.54	2.76	2.6	2.89
Hf	4	3.2	4	4.2	4.2	3.6	3.4	3	3.5	3.2	3.5	4	3.5	3.3
Ho	0.18	0.16	0.18	0.32	0.79	0.29	0.29	0.16	0.28	0.17	0.29	0.29	0.24	0.27
La	17.3	18.3	22.3	18.6	26.5	23.1	20.2	21.3	23.5	17.2	19.2.1	27.7	18.2	22.8
Lu	0.05	0.05	0.05	0.12	0.36	0.09	0.11	0.05	0.11	0.06	0.1	0.1	0.08	0.08
Mo	4	4	4	4	5	3	3	2	3	3	3	5	5	3
Nb	7.5	8.1	7.26	9.3	9.35	9.23	8.36	7.5	8.14	9	10	10.3	9.9	10.7
Nd	17	13.2	16.6	20	22.4	19.6	19.2	10.7	17.6	13.3	16.6	19.5	18.2	17.8
Ni	10	7	12	9	9	13	8	11	9	6	7	12	11	8
P	956	745	852	890	1255	958	1036	769	962	1950	1974	1325	1150	1856
Pb	14	16	15	14	12	15	17	13	16	15	16	17	15	19
Pr	5.36	3.92	5.23	5.64	5.93	5.74	5.62	3.2	5.09	4.13	4.88	5.6	5.29	5.04
Rb	47.7	51.3	45.9	42.9	83.1	46.9	52.7	43.6	52	54.1	55.2	48	48	54.9
Sm	2.39	3.1	3.37	3.28	4.23	3.13	3.25	2.67	3.78	2.2	2.77	4.96	2.81	2.85
Sr	910	850	850	960	850	890	870	920	820	895	925	847	820	850
Ta	0.9	0.6	0.9	0.7	0.7	0.7	0.8	0.5	0.7	0.7	0.7	0.8	0.7	0.8
Tb	0.25	0.21	0.25	0.38	0.68	0.33	0.33	0.2	0.31	0.23	0.32	0.34	0.3	0.31
Th	6.25	3.58	4.25	4.2	3.1	5.3	5.51	4.95	6.13	4.56	5.36	5.61	4.56	3.24
Ti	1858	1499	1918	2458	3956	2398	2278	1618	2278	1618	2218	2697	2278	2278
Tm	0.07	0.07	0.08	0.12	0.34	0.1	0.1	0.06	0.12	0.06	0.1	0.11	0.09	0.11
U	3.11	2.51	3.17	2.07	3.32	2.52	2.98	2.31	2.84	3.41	2.93	2.6	2.54	3
V	28	23	27	48	133	51	36	27	52	26	50	61	53	57
W	3	4	10	13	5	14	3	6	7	3	7	5	4	8
Y	9.2	8.3	7.5	8.2	9.3	7.7	7.8	8.4	8	9.5	7.8	7.4	8.3	7.3
Yb	0.56	0.69	0.57	0.74	2.27	0.65	0.72	0.65	0.71	0.43	0.67	0.71	0.75	0.71
Zn	75	52	65	56	75	58	54	56	58	41	65	60	54	53
Zr	48	45	51	56	78	75	62	62	53	71	76	52	82	54

In andesites, plagioclase is the most prominent light mineral, which accounts for about 30 to 50% of phenocrysts that show zonation and sieve texture (Fig 3). In dacitic specimens, the plagioclase forms more than 40 % volume of the rock. Quartz is also present as coarse-grained amorphous crystals with embayment corrosion in the felsitic groundmass. The ferromagnesian minerals in both andesitic and dacitic rocks include amphibole and biotite phenocrysts (5 to 10%) which usually show opacification evidence (Fig 3).

The predominant process in the hornblendes of the region is opacification. This phenomenon is due to the formation of metal minerals such as titanium magnetite, magnetite, and ilmenite. One of the conditions that cause hornblende instability is pressures of less than 1 kb, even in water-saturated systems, if it has been experimentally proven that the release of magma gas due to pressure reduction causes instability of the amphibole, replacement, and growth of the reaction margin in it. Some researchers (Nelson and Montana 1992; Mc Birney 2007) believe that the opacification reactions may be due to hornblende oxidation during magma ejection, reduced oxygen fugacity, and the formation of a volcanic dome.

The most important microscopic feature of the minerals of the dacite-andesitic rocks is the presence of sieve texture. Disequilibrium textures, particularly the coarse sieve texture of plagioclase, are common in orogenic volcanic rocks. The textures are usually interpreted as resulting from magma mixing, but they may occur by rapid decompression, where heat loss is minor relative to the ascent rate. The occurrence of the sieved textures, the Corrosion gulf of quartz, and the oscillatory zoning of plagioclases reveal magmatic contamination in the area (Fig 3).

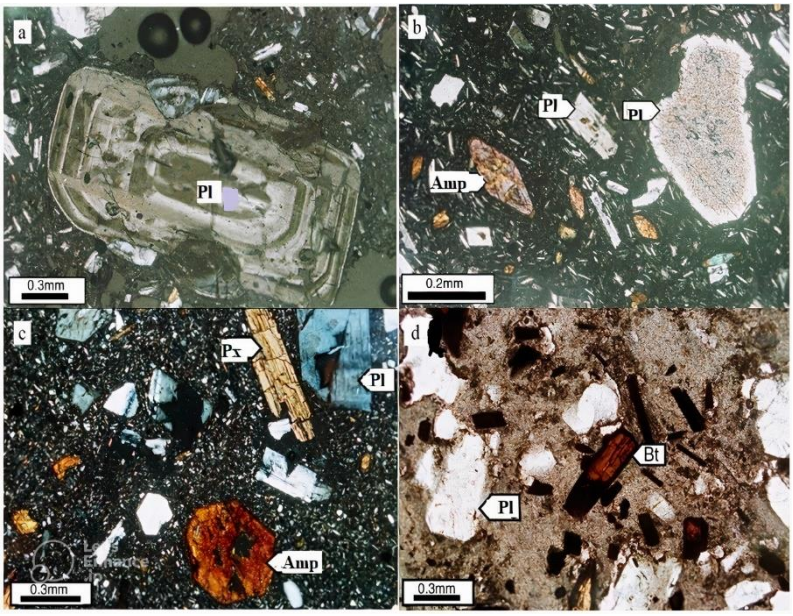

Fig 3. a) Full zoning plagioclase in the groundmass of the quartz-rich microcrystals and plagioclase-rich in andesite (XPL) b) Embayment margin in the plagioclase crystals in a microlithic groundmass of the andesite (XPL) c) Opacitation of amphibole mineral in dacite (XPL) d) Opacitized biotite in the dacite (PPL), Abbreviations for minerals are from Whitney and Evans (2010).

textural properties are stated, can be caused by alteration of magma composition due to contamination and Assimilation (Mc Birney 2007), reduction of magma pressure through its rise (Nelson and Montana 1992), increasing of vapor water pressure due to rapid ascension, and separation of magma in a single phase (Blat and Tracy 1995) or elevation of magma temperature as a result of hotter magma entering the reservoir or increasing its temperature due to magma outflow and oxidation, and it is visible after reaching the surface of the earth (Gill 1981).

4.2. Geochemistry

Geochemical results of the rocks southwest of Bostanabad show that they are the andesite and dacite in the total alkaline oxides vs. silica diagram (TAS; Le Bas et al. 1986). The dacite rocks are more abundant in all three studied massives (Arvane Mountain, Buick Dagh, and Kappan Dagh), (Fig 4). In the K_2O vs. SiO_2 diagram, the dacite-andesitic rocks of the regions are plotted in medium to high-K calc-alkaline fields (Peccerillo and Taylor 1976) (Fig 5). With minor elements, the studied series of calc-alkaline rocks with medium to high potassium are also evaluated (Peccerillo and Taylor 1976; Hastie et al. 2007). In the spider diagram (Fig 6), the rare earth elements normalized to the chondrite (Sun and Mc Donough 1989) of the resulting pattern show a certain negative slope from the LREE elements to the HREE elements. The diagram becomes much smaller and flatters towards the HREE (Fig 6). This pattern, together

with the positive anomaly Gd and the negative Eu anomaly, can be the result of prior crystallization and separation of calcium plagioclase, high fugacity CO_2/H_2O ratio and the presence of garnet in the material is the source of magma that produces these rocks. Of course, the relatively low severity of this negative anomaly can be due to subtraction and crustal contamination.

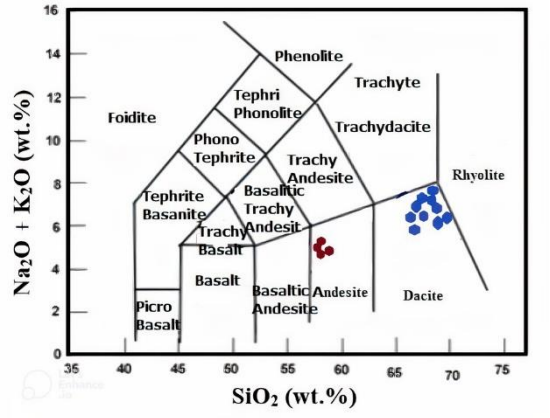

Fig 4. In the TAS diagram (Le Bas et al. 1986), the Miocene-Pliocene volcanic rocks of the southwest of Bostanabad plot in the dacite and andesite fields.

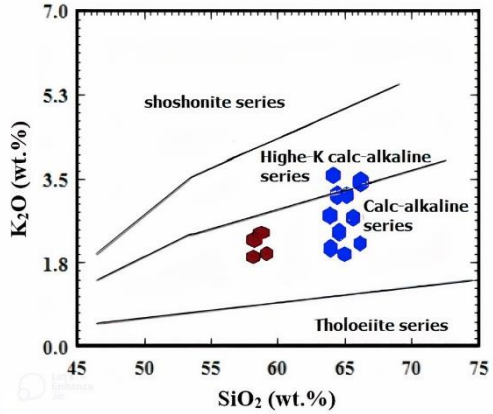

Fig 5. In the SiO_2 vs. K_2O diagram, the Miocene-Pliocene volcanic rocks southwest of Bostanabad are plotted in the medium to the high-K-calc-alkaline range, (Peccerillo and Talor 1976).

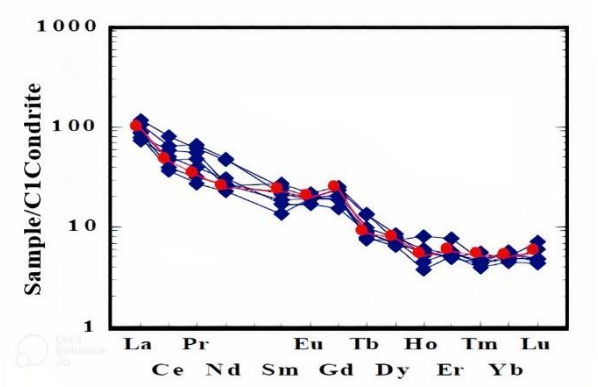

Fig 6. the chondrite-normalized diagram (Sun and Mc Donough 1989) for the Mio-Pliocene dacite-andesitic rocks of the southwest of Bostanabad concerning the inter-oceanic ridge basalts.

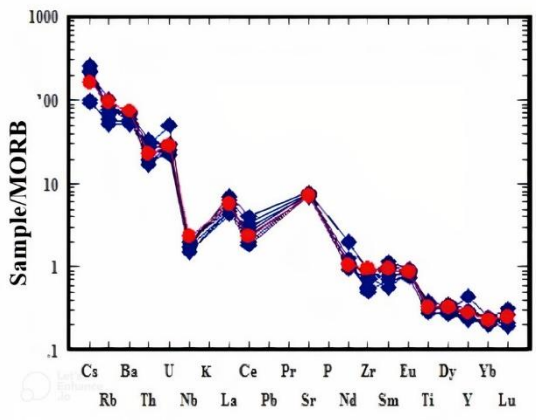

Fig 7. the trace element spider diagram normalized to MORB (Sun and Mc Donough, 1989) for the Mio-Pliocene dacite-andesitic rocks of the southwest of Bostanabad.

In Zr versus Zr / Y (Pearce et al. 1989) and La / Yb vs. Th / Yb (Condie 1989) diagrams, the samples are plotted in an active continental margin environment (Figs. 8 and 9). Also, values of Ba/Nb>100 and at Ba/Ta>500 of the dacitic-andesitic samples indicate an active continental margin environment (Ba/Nb >28 and Ba/Ta >450, respectively; Fitton et al. 1997). The Ni vs. Cr diagram revealed (Tsuchiya et al. 2005) that melting due to oceanic crust slabbing played a key role in the production of volcanic rocks southwest of Bostanabad (Fig 10). In addition, a similarity of magma composition of volcanic

The pattern of rare-element samples normalized to the Mid-Oceanic Ridge Basalts (MORB) indicates enrichment of the LILE (Ba, K, Pb, Rb, Sr, and Th) and depletion in the HFSE (Hf, Nb, Ta, Y, Yb, and Zr) (Fig 7). In this diagram, there is a clear negative anomaly for Nb, Ti, and Ta indicating the formation of the rocks in a subduction environment (Gill 1981; Wilson 1989).

massives of this region with crustal composition (Fig 11) indicates contamination of the magma with crust (Wang et al. 2008).

5. Discussion

Volcanic rocks and Subvolcanic-deep massives of the southwest of Bostanabad have MgO <3%, SiO_2> 57%, low Y (Y <13), and Yb <1.4. Heavy Rare Earth Elements (HREE) and high Ba/La, $(La / Yb)_N$>12, high Sr value (Sr> 400), and Sr / Y > 40 indicate adakitic properties

(Defant and Drummond 1993; Sterm and Kilian 1996). In the Sr/Y vs. Y diagram (Defant and Drummond 1993), the samples are in the adakite range (Alishah 2011a; Torkian et al. 2019). According to Defant and Drummond (1990), adakitic magmas originate from the melting of warm and young oceanic crust. While other researchers have suggested that adakites can be formed in other ways: (a) magmatic separation (Castillo 2012), (b) melting of hydrous peridotites (Martin et al. 2005; Stern and Hanson 1991), (c) mixing of basaltic magma with crust-derived felsic magma (Guo et al. 2007) and (d) partial melting of the homogeneously thick lower continental crust, (Xu et al. 2002; Guo et al. 2007; Foley et al. 2013).

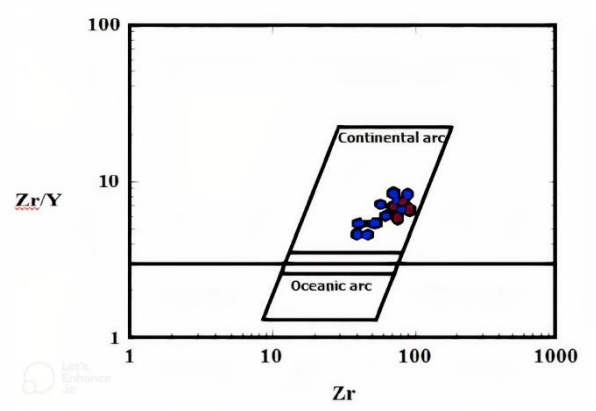

Fig 8. Zr versus Zr / Y (Pearce et al. 1989) separates the continental margin environment from oceanic arcs. Dacite-andesitic Mio-Pliocene rocks are located in the southwest of Bostanabad on the continental active margin.

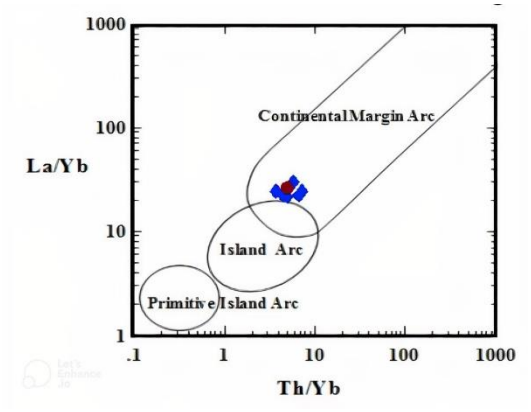

Fig 9. Th / Yb vs. La / Yb diagram separating the primary arcs from the mature arc islands and continental margin arcs (Condie 1989). Dacite-andesitic Mio-Pliocene rocks Southwest of Bostanabad are on the continental margin.

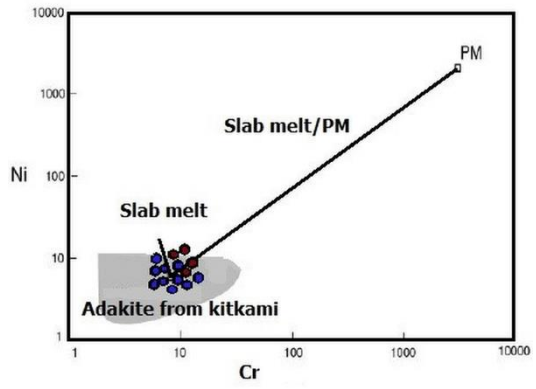

Fig 10. In Ni vs. Cr diagram (Tsuchiya et al. 2005), All samples are near the melt-derived slab and have a composition similar to that of Kitakami adakites, PM represents the primary mantle.

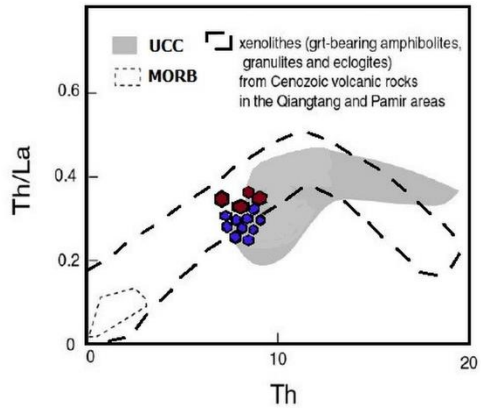

Fig 11. Th/La vs. Th diagram (Wang et al. 2008) xenolith range from Harker et al. (2005), Upper Crustal Composition (UCC) from Plank (2005), and Mid-Ocean Ridge Basalts (MORB) From Niu and Batiza (1997). All samples are within the continental crust and are similar to the composition of occlusal xenoliths and garnet-bearing amphibolites.

Adakites are divided into four groups: high silica adakites (HSA), low silica adakites (LSA), continental or potassium adakites, and Archaean adakites (Moyen 2009). High silica (HSA) adakites with MgO > 3%, SiO_2 > 56%, $La_N / Yb_N > 10$, high Sr content (Sr > 400), Sr / Y> 40 and low Y (Y < 18) and Yb (Yb < 19) are known to be compatible with the adakites proposed by Defant and Drummond (1990) and the adakites of Bostanabad region are similar to this type of adakites. These adakites are formed by partial melting of the metabasalts within the garnet stability field. Low silica adakites (LSA) contain 50 to 60% silica and have higher La / Yb and Sr / Y ratios (100 to 300 and 40 to 80, respectively). Experimental studies (Rapp et al. 2007) indicate that

metasomatized mantle melts (a mixture of peridotite + adakite) produce magma similar to the geochemical characteristics of low silica adakites (LSA). In addition to the above indications, there are significant geochemical differences between the two groups of high-silica adakites and low-silica adakites in the normalized chondrite diagrams. Low silica adakites have a more significant REE pattern than high silica adakites. Also, high silica adakites exhibit higher La / Yb and Sr / Y ratios than low silica adakites. The ratio of Yb / Lu in high silica adakites is about 10 and in low silica, adakites is about 5 (Moyen 2009).

Other researchers (Rapp et al. 2002; Ding et al. 2007; Xiao et al. 2007) consider high Sr / Y potassic rocks as continental adakites due to diverse petrogenetic processes. Archaean adakites resulting from the warm subduction and melting of the subducted melts are found in the Greenstone belt and are usually felsic and have low Na_2O and K_2O levels and show high Sr / Y ratios. Therefore, they are referred to as adakite (Moyen 2009). The Low and high silica adakites are formed in subduction-related environments when the subducted lithosphere is hot and buoyant (Peacock 1990; Morris 1995; Martin 1999). The high silica adakites are caused by the melting of subducted oceanic crust (Garnet-bearing metabasalts) and low-silica adakites are caused by partial melting of garnet-bearing metasomatic mantle wedges (Azizi et al. 2013). It is noteworthy that low-slip, rapid, young, and hot subduction produces abnormally high-temperature regimes (Torkian et al. 2019) that cause melting of slab and production of adakitic magmas. These adakites are real and classic. All the above-described features apply to the dacitic andesitic rocks of the southwest of Bostanabad have high similarity to classical adakites. Therefore, in this study, a comparison of the adakites with other adakites is discussed. In the Sr / Y vs. Y (Defant and Drummond, 1990) and Nb / Th vs. $(La / Sm)_N$ (Wang et al. 2004) discrimination diagrams of the adakites from acidic and intermediate rocks, the samples are within the adakitic field (Figs. 12 and 13). Subsequently, further diagrams were provided by Moyen (2009) to separate high-silica adakites from low-silica, Archean, and ordinary arc rocks (Modjarrad 2015). In these diagrams, the adakites of the southwest of Bostanabad were also identified as high silica (Fig 14).

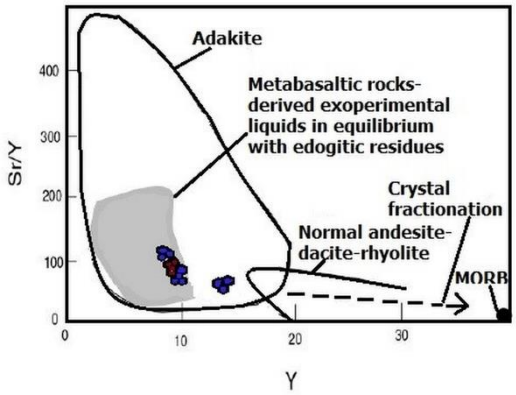

Fig 12. Y vs. Sr / Y (Defant and Drummond 1990) diagram, All samples of the southwest of Bostanabad are plotted in the Adakite range as well as the position of the meta-basaltic rocks in equilibrium with the experimental fluid of the eclogites is evaluated by Defant et al. (2002).

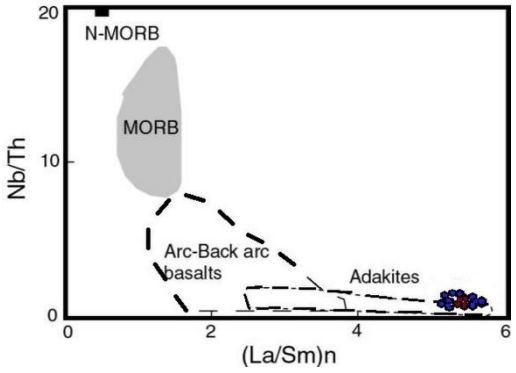

Fig 13. In Nb / Th vs. $(La/Sm)_N$ (Wang et al. 2004) diagram, the samples are all within the adakite range.

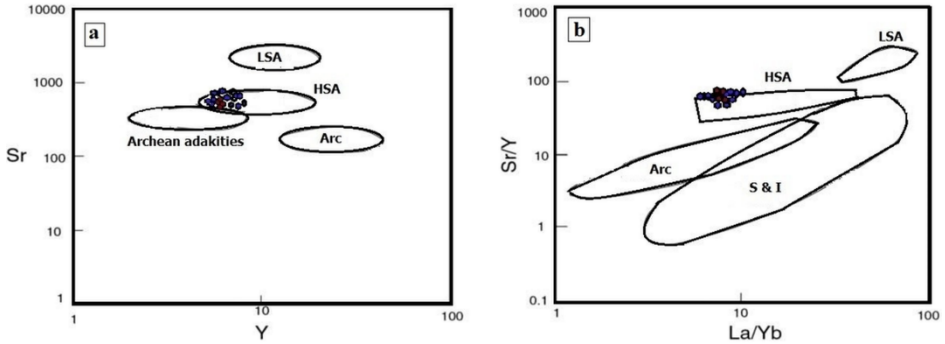

Fig 14. a, b) Diagrams for determining the types of low silica and high silica adakites (Moyen 2009). All samples of the southwest of Bostanabad are within the range of adakites (HAS).

To ensure the adakitic composition of the rocks in the Southwest of Bostanabad, the geochemistry of the samples was compared with the classic adakites introduced by Wang et al. (2011) in the Hohxil region of Tibet. Geoscientists believe that these adakitic dacites are the result of the partial melting of sediments on the subducted slab in the Songpan-Ganzi area. The composition of these dacites is similar to that of southwest Bostanabad. This is evident in the classical diagrams of adakites (Fig 15). Also, the REE pattern of these two groups (Fig 16) shows the same content and similarity of the ratios between rare earth elements. In La $_N$ / Yb $_N$ vs. Yb$_N$ (Defant and Drummond 1993) diagram, the samples are located in the garnet-amphibolite trend (with 25% partial melting), (Fig 17) indication of partial melting of garnet-bearing amphibolites as the main source of adakitic magmatism of the Neogene massives of Arvaneh Mountain, Buick Dagh, and Gapan Dagh in the southwest of Bostanabad. In bacillus adakites due to melting at high pressures, the eclogite is formed with garnet, clinopyroxene, and rutile minerals. Equlogite-origin equilibrium magma, due to the presence of rutile, shows higher Nb / Ta content than amphibolite origin (Foley et al. 2000; Foley et al. 2004; Schmidt et al. 2004; Avdeiko and Bergal-Kuvikas 2015). The average of this ratio in the samples is about 5.5 which is more compatible with the amphibolite origin. On the other hand, felsic and intermediate rocks that are in equilibrium with garnet have geochemical features such as high Al_2O_3, Ga and Sr / Y, low Lu, steep REE pattern, and no negative Eu anomaly due to lithospheric melting of the attached slab or partial melting of the lower crust granulite (Defant and Drummond 1990; Teklay and Mezger 2001; Eyuboglu et al. 2018; Eyuboglu et al. 2012; Sarem et al. 2021). Most adakitic magmas have been reported from the active margin of the Pacific Ocean concerning subduction. These magmas have been produced in environments where the younger oceanic lithosphere is younger than 20 million years, and the submerged plate is located 70 to 90 km below the volcanic arc (Morris 1995). Geochemical data of subduction-related magmas, collected by Defant and Drummond (1990), show that there is a universal agreement between the age of the subducted lithosphere and the composition of calc-alkaline magmas.

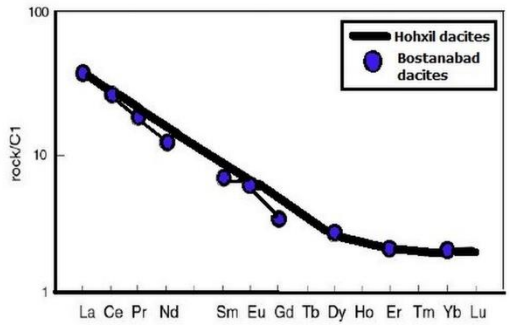

Fig 15. Normalized REE pattern of the southwestern Bostanabad and the Hohxil dacites relative to C1 (Sun and Mc Donough 1989).

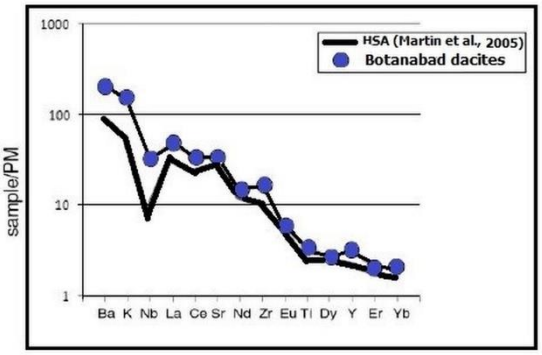

Fig 16. Comparison of variation pattern of rare earth elements of the rocks of the southwestern Bostanabad with HSA type (Martin et al. 2005). Normalization is based on primitive mantle values (Taylor and Mc Lennan 1985).

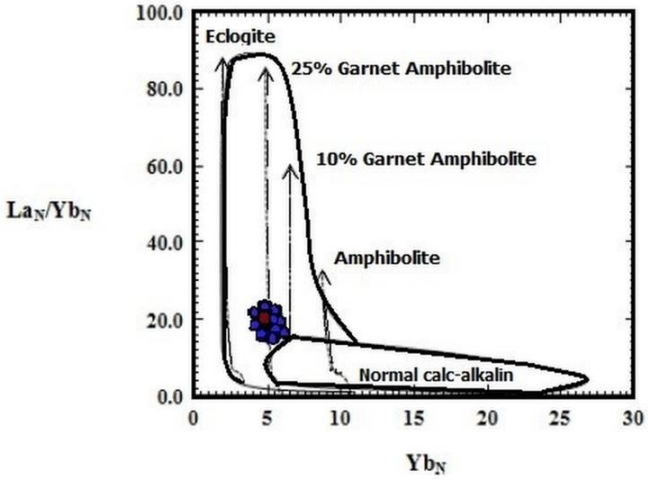

Fig 17. LaN/YbN vs. YbN diagram (Defant and Drummond 1993) and the position of the Mio-Pliocene dacite-andesitic rocks of the southwest of Bostanabad in the Garnet-Amphibolite range (Symbols as in Fig 5).

However, multiple subduction patterns and the occurrence of other adakites in different tectonic environments led Murray et al. (1996) to suggest that subducting plate melting is also possible in older oceanic crust. Castillo (2012) also suggested that partial melting of the lower crust because of infiltration of basaltic magma into the sub-lithosphere could lead to the formation of adakitic magma. Considering the high prevalence of adakites in subduction environments, it can be concluded that the thermodynamic conditions of the subduction system play a major role in melting the subduction plate (Shabanian et al. 2012; Jalili et al. 2015). Geochemical evidence thus suggests that dacites originate from basaltic crustal melting under pressure and heat conditions in which garnet and amphibole are stable and the plagioclase disappears. The Azerbaijan region has a thinner crustal thickness before the collision of the Arabian and Asian continents than at present (Dehghani and Markis 1993). The maximum crustal thickness, the thickness during the two continents' collision, is estimated to be 50 km in the study area (Afsari et al. 2011) so the lower crust in this region did not have sufficient thickness to convert eclogite or garnet-amphibolite components. On the other hand, according to research by Kay (1978), Defant and Drummond (1990), and Martin and Rollinson (2005) for adakitic compounds, the most important chemical properties of adakitis are Sr / Y> 40 and $(La / Yb)_N > 12$. Which is similar to the chemical composition of the rocks southwest of Bostanabad. With the explanations above, the development of the adakite magmatism in the region is as follows: Subduction of oceanic crust of Neotethys beneath central Iran and release of fluids in the mantle and metasomatization of upper deposited in the trench and accretionary wedge beneath central Iran causing volcanism and plutonism of calc-alkaline, alkaline, and shoshonitic in pre-Cretaceous age which may be due to their being covered by younger magmatic activities. The collision between the Arabian and Eurasian plates started in the early Miocene after the Neotethys Ocean was subducted beneath Eurasia (Dilek and Altunkaynak 2009).

Controversy exists in the literature about the timing of the closure of Neo-Tethyan along the Zagros suture. Some authors infer a late cretaceous age for continental collision (Berberian and Berberian 1981; Alavi 1994). A late Cretaceous age for continent-continent collision comes from the timing of the ophiolite emplacement, i.e. age of the youngest pelagic fossils involved in the Zagros ophiolites. However, this age has been shown to merely reflect the timing of ophiolite abduction due to the collision of the passive margin of Zagros-Oman an offshore intra-oceanic area (Berberian 1987), while a vast area of oceanic lithosphere still existed to the north of Zagros (Dercourt et al. 1986) yet to be subducted under Central Iran during the Tertiary. An alternative idea is that continental collision along the Zagros suture occurred in the Miocene (Berberian et al. 1982; Sengor and Natalin 1996; Sengor 1988). Paleo-ceanographic constraints derived from carbon and oxygen isotopic data indicate that Neo-Tethys had a connection with the northern Indian Ocean until 14Ma (Woodruff and Savin 1989). This factor supports the Miocene reconstruction of Neo-Tethys by Sengor and Natalin (1996) and is independent of regional geological evidence. The existence of widespread shallow marine and limited deep-marine Paleocene to Miocene sediment in Zagros sub-zones is consistent with the south arm of the Tethys remaining open into Miocene (Mohajjel et al. 2003) Opening of the Red Sea and the Gulf of Aden resulted in rotation of the Arabian plate concerning Africa (Nubia and Somalia) since 30 Ma (Bonatti 1987; Hempton 1987; Guiraud and Boswoeth 1999). This plate movement was responsible for oblique convergence between the Arabian plate and Central Iran and the final closure of Neo-Tethys.

Adakite studies have generated some confusion because (1) the definition of adakite combines compositional criteria with a genetic interpretation (melting of subducted basalt), (2) the definition is fairly broad and relies on chemistry as its distinguishing characteristic, (3) the use of high pressure melting experiment results on wet basalts as unequivocal proofs of slab melting and (4) the existence of adakitic rocks with chemical characteristics similar to adakites but are unrelated to slab melting. Other studies have shown that adakitic rocks and a number of the previously reported dates are produced through melting of the mafic lower crust or ponded basaltic magma, high-pressure crystal fractionation of basaltic magma, and low-pressure crystal fractionation of basaltic magma plus magma mixing processes in both arc or non-arc tectonic environments. Despite the confusing interpretations of the petrogenesis of adakite and adakitic rocks, their investigations have enriched our understanding of material recycling at subduction zones, crustal evolutionary processes, and economic mineralization (Jamali and Mehrabi, 2015; Ashrafi et al. 2018; Nazemi et al. 2019; Khalilzadeh et al. 2020)

Petrological studies carried out in the Central Iranian Magmatic Belt (CIMB) indicate that post-collisional magmas exhibit various geochemical enrichment signatures (Khodami 2019; Khodami et al. 2010). The significant character of post-collisional magmatism in this area indicates the progressive evolution of magmatic products from subalcalin to alkaline composition. A conspicuous characteristic of the alkaline phase is contemporaneous mafic alkaline melts including melafoidites and alkali-basalts (Hassanzadeh 1993). The onset of post-collisional magmatism in the late Plio-Pleistocene in this region will have adakitic geochemical signatures, indicating the role of slab melting after subduction has stopped. The temporal and spatial relationship of the studied adakitic rocks may be attributed to slab roll-back and possibly break-off subducted Neo-Tethyan oceanic lithosphere beneath the Central Iranian Continental Microplate (CICM). Slab

break-off may have led to thermal perturbation resulting in melting of detached slab and metasomatism of the mantle in Central Iran during the post-collisional event. The ascent of slab-derived magmas through the thickened continental crust in this region could have been the cause of crustal contamination resulting in high Rb / Sr ratios and an increase of K_2O, Th, and Y contents due to assimilation and fractional crystallization (AFC) processes. Evidence for AFC processes is marked by Enrichment of K_2O over Na_2O or incompatible LILE enrichment such as Rb, Th, and Ba over HFSE like Sr (Esperanca 1992). The values of radiogenic Sr(0.704 to 0.705) and ἐNd (+1.3 to +1.4) for these rocks respectively indicate assimilation, fractionation, and crystallization processes were involved (Moradian 1997), this isotopic composition of adakites are similar to MORB (Martin 1999).

Partial melting of the isolated oceanic crust caused by fractures and deep erosion faults in the continental crust probably produced acidic calc-alkaline magmas in the Azarbaijan region, especially the adakites in the southwest of Bostanabad (Alishah 2011b; Shabanian et al. 2012; Dalavari and Shahkeri 2016). The alkaline magmas of the area (Islamic Island) are most likely the result of highly metasomatized mantle partial melting with a low partial melting rate and calc-alkaline magmas are a result of partial melting rate or partial melting of the Neotethys oceanic crust. Fractures and faulting with east-west and northwest-southeast trends have played a major role in the final replacement of rocks southwest of Bostanabad. This model is used to produce high silica adakites magmas in other parts of the UDMB (Jahangiri, 2007; Ghadami et al. 2008; Omrani et al. 2008; Modjarrad 2015) as well as similar magmas in other parts of Iran (Nasrabady et al. 2015; Dalavari and Shahkeri 2016). In general, the geochemical properties of the samples are similar to the high-silica adakites (HSA). High ratios of Sr/Y and $(La/Yb)_N$ indicate the presence of amphibole and a small amount of garnet as stable phases in the source region of magma and it seems that the parent magma of studied adakite rocks is formed from the partial melting of the thickened lower continental crust.

The distribution of similar-age adakites in the NW Iran and E Pontides of Turkey suggests that these melts formed similarly. Upwelling of hot asthenosphere due to Neotethys slab rollback led to partial melting of lower continental crust calc-alkaline mafic rocks and/or amphibole fractionation from mafic magma produced K-rich adakitic rocks in eastern Turkey and NW Iran during the late Paleocene (Azizi et al. 2019).

6. Conclusions

The Mio-Pliocene volcanic rocks of the southwest of Bostanabad are dacite and andesite and their main minerals include plagioclase and amphibole in glassy to fine-grained texture with moderate to high calc-alkaline nature. In magmatic series diagrams, the samples are calc-alkaline. The studied variation pattern of rare and rare earth elements normalized to chondrite and primary mantle indicates enrichment of these rocks by LREE and LILE, deprived of REE elements such as Nb, Ce, Zn, and Ti, and High Field Strength Elements (HFSE), and the negative anomaly is Nb and Ti in these rocks, with the position of the samples on the diagrams indicate the formation of the rocks in a subduction-related environment at the active continental margin. Also, the rocks have higher values of La / Yb, SiO_2, and Sr / Y and lower values of MgO, Y, and Yb than conventional calc-alkaline volcanic rocks. These rocks in the discrimination diagrams are the calc-alkaline rocks in the adakite range. Due to the amounts of Sr, Si, Y, and heavy rare earth elements, absence of negative europium anomaly, rare element pattern, and diagrams of adakites, Mio-Pliocene rocks Southwest of Bostanabad are high silica adakites. They are comparable to adakites such as the post-collisional Plio-Pleistocene adakitic volcanism in the Central Iranian Volcanic Belt and Tibetan Hohxil that appear in the region as a single volcanic belt. The Southwest of Bostanabad adakite composition is just like the classic adakite composition. The variations in K_2O, LILE, and HFSE contents in comparison with modern adakites can be attributed to fractionation and crystallization processes. Based on geochemical data, the origin of these rocks is garnet-amphibolite with the residual phase of garnet and amphibole with a titanium phase. The garnet-amphibolite source rock that mainly contains high-grade metamorphic rocks, may have been caused by the continued subduction of the Neotethys oceanic lithosphere or its fragment and its melting in the Miocene-Pliocene produced high silica adakites magma and it formed dacite-andesitic rocks in the southwestern Bostanabad. Numerous genetic models can explain the formation of compositionally heterogeneous adakites, and therefore the use of the term adakite requires caution in their geodynamic interpretation. The occurrence of adakitic among the post-collisional magmatic rocks could represent the first magmatic products after the cessation of Neotethys subduction in the volcanic belt of Iran.

Acknowledgments

I would like to thank my dear professors Dr. Mansour Vosoughi Abedini and Dr. Mansour Ghorbani who patiently and compassionately helped me in this research by providing useful comments and suggestions.

References

Afsari N, Sodoudi F, Taghizade FF, Ghassemi MR (2011) Crustal structure of Northwest Zagros (Kermanshah) and Central Iran (Yazd and Isfahan) using teleseismic Ps converted phases. *Journal of Seismology* 15: 341–353.

Agard P, Omrani J, Jolivet L, Whitechurch H, Vrielynck B, Spakman W, Monie P, Meyer B, Wortel R (2011) Zagros orogeny, A subduction-dominated process, *Geology Magazines* 10: 1-34.

Aghanabati A (2004) Geology of Iran, Geological Survey of Iran, Tehran.

Aghazadeh M, Emami MH, MoineVaziri H, Rashidnezhad Omran N, Castro A (2011) Post-collisional shoshonitic, C-type Adakitic and lamprophyric plutonism in the Khankandi Pluton, Arasbaran (NW Iran). *Geosciences* 20(78): 173-188.

Ahmadzadeh G, Jahangiri A, Mojtahedi M, Lentz D (2011) Petrogenesis of Plio-Quaternary post-collisional adakitic rocks in Northwest Marand. *Iranian Journal of Crystallography and Mineralogy* 18: 709-722.

Alavi M (1994) Tectonics of Zagros orogenic of Iran, new data and interpretation, *Journal of Tectonophysics* 229: 211-238.

Alishah FP (2011) Geochemistry of adakitic composition of Sahand volcano at the south of Tabriz, 30th symposium of Erath Sciences, Geological Survey of Iran, Tehran (in Persian).

Alishah FP (2011) Petrology, Geochemistry and Petrogenesis of Volcanic Rocks in the East and Southeast of Sahand Volcano with Special Reference to the Pyroclastic Rocks, Ph. D thesis, University of Tabriz, Iran, 198pp, (in Persian).

Alishah FP, Ameri A, Jahangiri A, Mojtahedi A, Keskin M (2012) Petrology and geochemistry of volcanic rocks from the south of Tabriz (Sahand volcano). *Petrology* 9(1): 37-56 (in Persian).

Amel N (2008) Petrology and Petrogenesis of Plio-Quaternary magmatic rocks of Azerbaijan- NW Iran, Ph. D thesis, University of Tabriz, Iran 188.

Annen C, Blundy JD, Sparks RSJ (2006) The genesis of intermediate and silicic magmas in deep crustal hot zones, *Journal of Petrology* 47: 505-539.

Ashrafi N., Jahangiri A., Hasebe N., Eby G.N (2018) Petrology, geochemistry and geodynamic setting of Eocene-Oligocene alkaline intrusions from the Alborz-Azerbaijan magmatic belt, NW Iran, *Journal of Chemie der Erde* 78: 432-461.

Avdeiko GP, Bergal-Kuvikas OV (2015) The Geodynamic Conditions for the Generation of Adakites and Nb_Rich Basalts (NEAB) in Kamchatka, *Journal of Volcanology and Seismology* 9 (5): 295–306.

Azizi H, Asahuru Y, Motohiro T, Takemura K, Razyani S (2013) The role of the heterogenetic mantle in the genesis of adakites northeast of Sanandaj, northwestern Iran, *Chemie der Erde* 74:87-97.

Azizi H, Robert J. Gültekin Topuz S, Yoshihiro A, Shafaii Moghadam, H (2019) Late Paleocene adakitic granitoid from NW Iran and comparison with adakites in the NE Turkey: Adakitic melt generation in normal continental crust, *Lithos*, 346–347.

Behrouzi A, Amini Fazl A, Amini Azar B (1997) Geological Survey of Iran, 1:100,000 Series, Sheet 5265, Bostanabad.

Berberian E (1987) Oceanic evolution, *rifting or drifting in the Red Sea. Nature330*: 692-693.

Berberian F, Berberian M (1981) Tectono-plutonic episodes in Iran. In, Zagros, Hindokosh, Himalaya Geodynamic Evolution (Eds Gupta, H K, Delany F M) 5-32. *Journal of American Geophysical Union, Washington.*

Berberian F, Muir ID, Pankhurst RJ, Berberian M (1982) Late Cretaceous and early Miocene Andean type plutonic activity in northern Makran and central Iran. *Journal of Geological Society of London*139: 605-614.

Bilici O, Kolaylı H, Kalkan E, Bilici T, Yarbaşı N (2020) Petrographic and Geochemical Fingerprints of Sub-Volcanic Dykes and their Host Harzburgites from the Ulaş Ultramafics (Sivas, Turkey), International *Journal of Earth Science Knowledge and Applications* 2(1):1-12.

Bina M, Arian MA, Pourkermani M, Bazoobandi MH, Yazdi A (2020) Study of the petrography and tectonic settings of sills In Lavasanat district, Tehran (north of Iran), *Nexo Revista Cientifica*, 33(2), 286-296.

Blatt H, Tracy R (1995) Petrology: igneous, sedimentary and metamorphic, W H, Freeman book Company, New York.

Bonatti E (1987) Oceanic evolution, rifting or drifting in the Red Sea? *Nature* 330: 692-693.

Castillo PR (2012) Adakite petrogenesis, *Lithos* 134: 304-316.

Condie KC (1989) Geochemical changes in basalts and andesites across the Archean-Proterozoic boundary, identification, and significances, *Lithos* 23: 1-18.

Dalavari Koshan M, Shahkeri A (2016) Taftan volcanic rocks: evidence of Pseudo-adakit magmatism in Makran magmatic arc, *Quaternary journal of Iran* 2(1): 1-14.

Davoudzadeh M, Lammerer B, Weber-Diefenbach K (1997) Paleogeography, Stratigraphy, and tectonics of the tertiary of Iran. *Neues Jahrbuch Geologie Palaontologie Abhandlungen* 205: 33–67.

Defant MJ, Drummond MS (1990) Derivation of some modern arc magmas by melting of the young, subducted lithosphere, *Nature* 374: 662-665.

Defant MJ, Drummond MS (1993) Mount St. Helens: potential example of the partial melting of the subducted lithosphere in a volcanic arc. *Journal of Geology* 21: 547-550.

Dehghani GA, Markis J (1993) The gravity field and crustal structure of Iran, In Geodynamic project (Geotraverse) in Iran, Geological Survey of Iran, *Report* 51:51-68.

Dercourt J, Zonenenshain L, Ricou LE, Kazmin G, Lepichon X, Knipper AL, Grandjacquet C, Sbotshikov IM, Geyssant J, Lepvrier C, Pechersky DH, Boulin J, Sibuet JC, Savostin LA, Sorokhtin O, Westphal M, Bazhenov ML, Lauer JP, BijuDuval B (1986) Geological evolution of the Tethys belt from the Atlantic to Pamirs since the Lias. *Tectonophysics* 123: 241-315.

Dilek Y, Altunkaynak S (2009) Geochemical and temporal evolution of Cenozoic magmatism in western Turkey, Mantle response to a collision, slab breakoff, and lithospheric tearing in an orogenic belt, (Eds. Van Hinsbergen, DJJ, Edwards MA, Govers R) Collision

and Collapse at the Africa-Arabia-Eurasia Subduction Zone, *Geological Society of London Special Publication* 311: 213-233.

Ding L, Kapp P, Yue Y, Lai Q (2007) Postcollisional calc-alkaline lavas and xenoliths from the southern Qiangtang terrane, *Central Tibet. Earth and Planetary Science Letters* 254: 28-38.

Esperanca S, Crisci M, de Rosa R, Mazzuli R (1992) The role of the crust in the magmatic evolution of the island Lipari (Aeolian Islands. Italy). *Contributions to Mineralogy and Petrology* 112: 450-462.

Eyuboglu Y, Dudasb FO, Santosh M, Eroglu-Gumruk T, Akbulut K, Yi K, Chatterjee N (2018) The final pulse of the Early Cenozoic adakitic activity in the Eastern Pontides Orogenic Belt (NE Turkey): An integrated study on the nature of the transition from adakitic to non-adakitic magmatism in a slab window setting, *Journal of Asian Earth Sciences157*:141-165.

Eyuboglu Y, Santosh M, Yi K, Bektaş O, Kwon S (2012) Discovery of Miocene adakitic dacite from the Eastern Pontides Belt and revised geodynamic model for the late Cenozoic evolution of the eastern Mediterranean region, *Lithos* 146-147: 218-232.

Fitton JG, Saunders AG, Norry MJ, Hardarson BS (1997) Thermal and chemical structure of the Iceland Plume. *Earth andPlanetary Science Letters* 153:197–208.

Foley FV, Pearson NJ, Rushmer T, Turner S, Adam J (2013) Magmatic evolution and magma mixing of Quaternary adakites at Solander and little Solander Islands, New Zealand, *Journal of Petrology* 54(4): 703–744.

Foley S, Tiepolo M, Vannucci R (2004) Growth of early continental crust controlled by melting of amphibolite in subduction zones, *Nature* 417: 832-840.

Foley SF, Barth MG, Jenner GA (2000) Rutile/melt partition coefficients for trace elements and an assessment of the influence of rutile on the trace element characteristics of subduction zone magmas, *Geochimica et Cosmochimica Acta* 64: 993-938.

Ghadami GR, Shahre-Babaki A, Mortazavi M (2008) Post-collisional Plio-Pleistocene adakitic volcanism in Central Iranian volcanic belt, geochemical and geodynamic implications, *Journal of Sciences Islamic Republic of Iran* 19: 223-235.

Ghaffari M, Rashidnejad-Omran N, Dabiri R, Chen B, Santos JF (2013) Mafic–intermediate plutonic rocks of the Salmas area, northwestern Iran: their source and petrogenesis significance. *International Geology Review* 55(16): 2016-2029.

Ghalamghash J, Schmitt AK, Chaharlang R (2019) Age and compositional evolution of Sahand volcano in the context of post-collisional magmatism in northwestern Iran: Evidence for time-transgressive magmatism away from the collisional suture, *Lithos* (344-345): 265-279.

Ghasemi A, Talbot CJ (2006) A new tectonic scenario for the Sanandaj-Sirjan Zone (Iran), *Journal of Asian Earth Sciences* 26:683-693.

Gill JB (1981) Orogenic andesites and plate tectonics, Springer, Verlag, Berlin.

Guiraud R, Boswoeth W (1999) Phanerozoic geodynamic evolution of northeastern Africa and northwestern Arabian platform. *Tectonophysics* 282: 39-82.

Guo F, Nakamuru EFW, Kobayoshi KLC (2007) Generation of Palaeocene adakitic andesites by magma mixing: Yanji Area, NE China. *Journal of Petrology* 48: 661-692.

Hacker BR, Luffi P, Lutkov V, Minaev V, Ratschbacher L, Plank T, Ducea M, Patiño Douceae A, McWilliams M, Metcalf J (2005) Near-ultrahigh pressure processing of continental crust, Miocene crustal xenoliths from the Pamir, *Journal of Petrology* 46: 1661-1687.

Hassanzadeh J (1993) Metallogenic and tectonomagmatic events in the SE sector of the Cenozoic active continental margin of Iran (Shahre Babak area, Kerman province), Ph.D. thesis, University of California, USA.

Hastie AR, Kerr AC, Pearce JA, Mitchell SF (2007) Classification of altered volcanic island arc rocks using immobile trace elements, development of the Th-Co discrimination diagram, *Journal of Petrology* 48: 2341-2357.

Hempton MR (1987) Constraints on Arabian plate motion and extensional history of the Red Sea. *Tectonic* 6: 687-705.

Jahangiri A (2007) Post-collisional Miocene adakitic volcanism in NW Iran, geochemical and geodynamic implications, *Journal of Asian Earth Sciences* 30: 433-447.

Jalili G, Nasir A, Hajaliogli R, Moayyed M (2015) Petrogenesis of adakitic Plio-Quaternary post-collision rocks, north of Sahand volcano (NW of Iran). *Journal of Petrology* 8(22): 157-172.

Jamali H., Mehrabi B (2015) Relationships between arc maturity and Cu-Mo-Au porphyry and related epithermal mineralization at the Cenozoic Arasbaran magmatic belt, *Ore Geology Reviews* 65:481-501.

Kay RW (1978) Aleutian Magnesian andesites, melts from subducted Pacific Ocean crust, *Journal of volcanology and Geothermal Research* 4: 497-522.

Keskin M (2003) Magma generation by slab steeping and break-off beneath a subduction accretion complex: an alternative model for collision-related volcanism in eastern Anatolia, Turkey, *Journal of Geophysical Research Letters* 30: 80-46.

Khalilzadeh H, Alipour S, Abedini A (2020) Investigation of adakitic feature and magmatic origin of mineralized monzonitic stock in the Niza area, northwest Iran. *Iranian Journal of Crystallography and Mineralogy* 28 (1) :3-16

Khodami M, (2019) Pb isotope geochemistry of the late Miocene–Pliocene volcanic rocks from Todeshk, the central part of the Urumieh–Dokhtar magmatic arc, Iran: Evidence of an enriched mantle source. *Journal of Earth System, Science* 128:167

Khodami M, Noghreyan M, Davoudian AR (2010) Geochemical constraints on the genesis of the volcanic rocks in the southeast of Isfahan area, Iran. *Arabian Journal of Geosciences* 3: 257–266.

Le Bas M, Le Maistre RW, Streckeisen A, Zanettin B (1986) A chemical classification of volcanic rocks based on the total alkali-silica diagram, *Journal of Petrology* 27: 745-750.

Maniar PD, Piccoli PM (1989) Tectonic discrimination of granitoids, *Geological Society of America Bulletin* 101: 635-643.

Martin H (1999) The adakitic magmas: modern analogs of Archaean granitoids. *Lithos* 46 (3): 411-429.

Martin H, Rollinson H, (2005) Geodynamic controls on adakite. TTG and Sanukitoid genesis: implications for models of crust formation. *Lithos* 79: 1-4.

Martin H, Smithies RH, Rapp RP, Moyen JF, Champion DC (2005) An overview of adakite, tonalite-trondhjemite-granodiorite (TTG) and sanukitoid, relationships and some implications for crustal evolution, *Lithos* 79(1-2): 1-24.

Mc Birney AR (2007) Igneous petrology. 3rd edition, Jones and Bartlett Learning, Burlington, Canada.

Modjarrad M (2013) Petrology and geochemistry of Bezow-Draghi area volcanic rocks, Urmia-NW Iran, research project final report, Urmia University, Urmia, Iran (in Persian).

Modjarrad M (2014) Petrology and geochemistry of the Bezow-Draghi volcanic rocks (Urmia), W Azarbaijan; introduction. *New Findings on Applied Geology* 16: 16-24.

Modjarrad M (2015) Geochemistry of Bezow-Draghi volcanic rocks, Urmia; adakitic magmatism in the Uromieh-Dokhtar magmatic belt, *Petrology* 21(1): 121-138.

Mohajjel M, Fergusson CL, Sahandi, MR (2003) Cretaceous-Tertiary convergence and continental collision, Sanandaj-Sirjan zone, western Iran. *Journal of Asian Earth Sciences* 21: 397-412.

Moine Vaziri H, Amine Sobhani E (1977) Volcanology and volcano sedimentology of Sahand region. Tarbiat-e-Moalem university, p: 55.

Moradian A (1997) Geochemistry, Geochronology and petrography of Feldspathoid Bearing Rocks in Urumieh Dokhtar Volcanic Belt, Iran Unpublished Ph. D thesis, University of Wollongong, Australia, 412 pp.

Morris JD (1995) Slab melting as an explanation of Quaternary volcanism and seismicity in southwestern Japan, *Geology* 23:395-398.

Moyen JF (2009) High Sr/Y and La/Yb ratios: the meaning of the adakitic signature, *Lithos* 112: 556-574.

Murray CG (1996) Zoned ultramafic complexes of the Alaskan type: Feeder pipes of andesitic volcanoes, *Geological Society of America* 132:35-313.

Nabavi M (1976) Perfect geology of Iran, Geological Survey of Iran, Tehran.

Nasrabady M, Rossetti F, Moin Vaziri H, R S, M M (2015) Petrogenesis of Adakitic Intrusion Bodies of the Ophiolitic Belt, NE Sabzevar, *Journal of Geoscience* 24(94): 183-196.

Nazemi E, Arian MA, Jafarian A, Pourkermani M, Yazdi A (2019) Studying The Genesis Of Igneous Rocks In Zarin-Kamar Region (Shahrood, Northeastern Iran) By Rare Earth Elements, *Revista Gênero e Direito* 8 (4): 446-466.

Nelson T S, Montana A (1992) Sive-textured plagioclase in volcanic rocks produced by rapid decompression. *American Mineralogy* 77: 1242-1249.

Niu Y, Batiza R (1997) Trace element evidence from seamounts for the recycled oceanic crust in the eastern equatorial Pacific mantle. *Earth Planet Science Letter* 148:471-484.

Noghreyan M, Khodami M, Davoudian A, Shabanian Brogeni N (2011) Petrogenesis of Pliocene-Quaternary volcanic rocks in Isfahan province, insight on adakite magmatism, *Iranian Journal of Crystallography and Mineralogy* 19: 451-462.

Omrani J, Agard P, Whitechurch H, Benoit M, Prouteau G, Jolivet I (2008) Arc-magmatism and subduction history beneath the Zagros Mountains, Iran: a new report of adakites and geodynamic consequences, *Lithos* 106:380-398.

Peacock SM (1990) Fluid processes in subduction zones, *Science* 248: 329-337.

Pearce JA, Harris NBW, Tindle AG (1989) Trace element discrimination diagrams for the tectonic interpretation of granitic rocks, *Journal of Petrology* 25: 956-983.

Peccerillo A, Taylor SR (1976) Geochemistry of Eocene calc-alkaline volcanic rocks from the kastamonu area, northern Turkey, *Contributions to Mineralogy and Petrology* 58: 63-81.

Plank T (2005) Constraints from Thorium/Lanthanum on sediment recycling at subduction zones and the evolution of the continents, *Journal of Petrology* 46(5): 921-944.

Rapp R, Xiao L, Shimizu N (2002) Experimental constraints on the origin of potassium-rich adakites in eastern China, *Acta Petrologica Sinica* 18: 293-302.

Rapp R, Yaxley G, Norman MD, Shimizu N (2007) Comprehensive trace element characteristics of experimental TTG and sanukitoid melts, In: Proceeding of the 6th International Hutton Conference on the origin of granitic rocks, Stellenbosch, South Africa.

Reichenbacher B, Alimohammadian H, Sabouri J, Haghfarshi E, Faridi M, Abbasi S, Matzke-Karasz R, Fellin MG, Carnevale G, Schiller W, Vasilyan D, Scharrer S (2011) Late Miocene stratigraphy, palaeoecology, and paleogeography of the Tabriz Basin (NW Iran, Eastern Paratethys). Paleogeography, Palaeoclimatology, *Palaeoecology* 311: 1–18.

Sarem MN, Abedini MV, Dabiri R, Ansari MR (2021) Geochemistry and petrogenesis of basic Paleogene volcanic rocks in Alamut region, Alborz mountain, north of Iran. *Earth Sciences Research Journal* 25(2): 237-245.

Schmidt GA, Shindell DT, Miller RL, Mann ME, Rind M (2004) General circulation modeling of Holocene climate variability. *Quaternary Science Reviews* 23: 2167-2181,

Sengor AMC, Altmer D, Cin A, Ustaomer T, Hsu KJ (1988) Origin and assemble of the Tethyside orogenic collage at the expense of Gondwanaland. In: AudleyCharls, M. G., Hallam, A. (Eds.), Gondwana and Tethys. *Geological Society of London*, 37: 19-181.

Sengor AMC, Natalin BA (1996) Paleotectonic of Asia: fragments of a synthesis. In Yin A, Harrison TM, (Eds.), The Tectonic Evolution of Asia Cambridge University Press, *Cambridge*, 486-640.

Shabanian E, Acocella V, Gioncada A, Ghasemi H, Bellier O (2012) Structural control on volcanism in intraplate post collisional settings: late Cenozoic to Quaternary examples of Iran and Eastern Turkey, *Tectonics* 31:13-30.

Sipahi F, Saydam Eker C, Akpınar I, Gucer MA, Vural A, Kaygusuz A, Aydurmuş T (2021) Eocene magmatism and associated Fe-Cu mineralization in northeastern Turkey: A case study of the Karadag skarn, *International Geology Review* 64: 1530-1555.

Stern CR, Kilian R (1996) Role of the subducted slab, mantle wedge and continental crust in the generation of adakites from the Andean austral volcanic zone, *Contributions to Mineralogy and Petrology* 123: 263-281.

Stern RA, Hanson GN (1991) Archean High-Mg granodiorite: a derivative of light rare earth element enriched monzodiorite of mantle origin. *Journal of Petrology* 32:201-238.

Stocklin J, Setudenia A (1971) Stratigraphic lexicon of Iran. Geological Survey of Iran, Tehran.

Sun SS, Mc Donough WF (1989) Chemical and isotopic systematics of oceanic basalts: implication for mantle composition and processes. In: Magmatism in the ocean basins (Eds. Sanders, A. D., and Norry, M. H.), *Geological Society of London* 42: 313-345.

Taylor SR, McLennan SM (1985) The composition and evolution of the continental crust: rare earth element evidence from sedimentary rocks, *Philosophical Transactions of the Royal Society of London* 381-399.

Teklay KA, Mezger K (2001) Geochemistry, geochronology and isotope geology of Nakfa intrusive rocks, northern thickened Neoproterozoic arc crust, *Journal of African Earth Sciences* 33(2): 283-301.

Torkian A, Furman T, Salehi N, Veloski K (2019) Petrogenesis of adakites from the Sheyda volcano, NW Iran. *Journal of African Earth Sciences* 150:194-204.

Tsuchiya N, Suzuki S, Kimura JI, Kagami H (2005) Evidence for slab melt/mantle reaction: petrogenesis of early Cretaceous and Eocene high-Mg andesites from the Kitakami mountains, Japan, *Lithos* 79: 179-206.

Vural A, Kaygusuz A (2021) Geochronology, petrogenesis and tectonic importance of Eocene I-type magmatism in the Eastern Pontides, NE Turkey. *Arabian Journal of Geosciences* 14: 467.

Wang Q, Li ZX, Chung SL, Wyman, DA, Sun YL, Zhao ZH, Zhu YT, Qiu HN (2011) Late Triassic high-Mg andesite/dacite suites from northern Hohxil, north Tibet: Geochronology, geochemical characteristics, petrogenetic processes, and tectonic implications, *Lithos* 126: 54-67.

Wang Q, Wyman DA, Xu JF, Wan YS, Li CF, Zi F, Jiang ZQ, Qiu HN, Chu ZY, Zhao ZH, Dong YH (2008) Triassic Nb-enriched basalts, magnesian andesites, and adakites of the Qiangtang terrane (Central Tibet): evidence for metasomatism by slab derived melts in the mantle wedge, *Contributions to Mineralogy and Petrology* 155: 473-490.

Wang Z, Wilde SA, Wang K, Yu L (2004) A MORB-arc basalt-adakite association in the 2.5 Ga Wutai greenstone belt: late Archean magmatism and crustal growth in the North China craton, *Precambrian Research* 131: 323-343.

Whitney DL, Evans BW (2010) Abbreviations for Names of Rock-Forming Minerals. *American Mineralogist*, 95: 185-187

Wilson M (1989) Igneous petrogenesis a global tectonic approach. 1st edition, Unwin and Hyman London.

Woodruff F, Savin SM (1989) Miocene deepwater oceanography. *Paleoceanography* 4: 87-140.

Xiao L, Zhang HF, Clemens JD, Wang QW, Kan ZZ, Wang KM, Ni PZ, Liu XM (2007) Late Triassic granitoids of the eastern margin of the Tibetan Plateau: geochronology, *petrogenesis and implications for tectonic evolution.* Lithos 96: 436-452.

Xu JF, Shinjo R, Defant MJ, Wang Q, Rapp RP (2002) Origin of Mesozoic adakitic intrusive rocks in the Ningzhen area of China: partial melting of delaminated lower continental crust, *Journal of Geology* 30: 1111-1114

Yadollahi R, Kananian A, Maanijou M, Sarjoughian F, Hassanpour Sh (2011) Genesis of adakitic magmatism in Masjed Draghi region in Julfa, eastern Azarbaijan, *Iranian Journal of Crystallography and Mineralogy* 19: 297-310.

Yazdi A, Shahhosseini E, Moharami F (2022) Petrology and tectono-magmatic environment of the volcanic rocks of West Torud–Iran, *Iranian Journal of Earth Sciences* 14 (1): 40-57.

Zhang L, Hu Y, Ling G, Ireland T, Chen Y, Ghang R, Sun S, Su N (2017). Adakitic rocks are associated with the Shilu copper-molybdenum deposit in the Yangchun Basin, South China. *Acta Geochim* 36(2): 132–150.